International Journal of Mechanical, Industrial and Aerospace Sciences
ISSN: 2517-9950
Vol:13, No:3, 2019

Surface Pressure Distribution of a Flapped-Airfoil for Different Momentum Injection at the Leading Edge

Mohammad Mashud, S. M. Nahid Hasan

Abstract**—**The aim of the research work is to modify the NACA 4215 airfoil with flap and rotary cylinder at the leading edge of the airfoil and experimentally study the static pressure distribution over the airfoil completed with flap and leading-edge vortex generator. In this research, NACA 4215 wing model has been constructed by generating the profile geometry using the standard equations and design software such as AutoCAD and SolidWorks. To perform the experiment, three wooden models are prepared and tested in subsonic wind tunnel. The experiments were carried out in various angles of attack. Flap angle and momentum injection rate are changed to observe the characteristics of pressure distribution. In this research, a new concept of flow separation control mechanism has been introduced to improve the aerodynamic characteristics of airfoil. Control of flow separation over airfoil which experiences a vortex generator (rotating cylinder) at the leading edge of airfoil is experimentally simulated under the effects of momentum injection. The experimental results show that the flow separation control is possible by the proposed mechanism, and benefits can be achieved by momentum injection technique. The wing performance is significantly improved due to control of flow separation by momentum injection method.

Keywords**—**Airfoil, momentum injection, flap and pressure distribution.

I. Introduction

IN an airplane, wings are at the most import part to fly, firstly none can think an airplane without wing. Wing is nothing but airfoil section with span wise extension. When the fluid flows over the wing, i.e. airfoil section lift and drag forces generated on the wing. Lift can be increased or decreased by changing the angle of attack but it has a limit. Drag force also depends on the airfoil section surface, fluid velocity and angle of attack. After a certain angle of attack, flow is separated from the wing surface and it results in sudden drop of lift force and at the same time drag force increase dramatically. Most of the aerodynamic researchers interested to control the flow separation on the surface of a wing, i.e. delaying the separation point. Whenever the separation delayed for a specific wing or airfoil section, the lift force increases as well as decreases the drag force. To calculate the lift and drag force, Rong et al. [1] presented correlations for inviscid fluid with all variables such as air density, velocity, viscosity, surface area, shape of airfoil, angle of attach and compressibility factor which is shown below.

Mohammad Mashud and S M Nahid Hasan are with the Department of Mechanical Engineering, Khulna University of Engineering & Technology, Khulna-9203, Bangladesh (e-mail: mdmashud@yahoo.com; engrsmnahidhasan@gmail.com).

$$L=1/2\rho U^2 S C_L \quad (1)$$

Total drag force D can be calculated by:

$$D=1/2\ \rho U^2 S C_D \quad (2)$$

Kandwal et al. [2] showed the dependency of pressure distribution on airfoil section for C_L and has done the simulation of inviscid flow over airfoil. The authors found that maximum pressure coefficient occurs at the point of stagnation which is natural and obey flow property. The velocity of fluid flow over the surface is maximum due to the geometry of the wing, consequently the upper surface pressure shows the negative magnitude, i.e. suction pressure. This pressure continues till stall and then the surface pressure becomes extremely adverse due to the effect of shear force along the flow field. For the reason of adverse pressure gradient, flow become reversed and tends to separate from solid boundary that decorates the lift generation but it increases the drag force. By this way, lift capability correlates the flow separation and such extension prevents the flow separation to reduce drag and increase lift [3].

At low Reynolds number, the flow the tendency of flow separation is higher, then high Reynolds number, which will induce serious effects on aerodynamic performances of airplanes during take-off and landing, and the maneuvering flight of some Unmanned Aerial Vehicles (UAVs). In order to suppress the flow separation and improve the aerodynamic performances of aircrafts, many kinds of control methods have been developed. Suction control is one of the most promising methods which have been investigated for decades. Vortex generators (VGs) are used to trigger this transition. Other devices such as vortilons, leading-edge extensions, leading edge cuffs, also delay flow separation at high angles of attack by re-energizing the boundary layer. Examples of aircraft which use VGs include the Embraer 170 and Symphony SA-160. For swept-wing transonic designs, VGs alleviate potential shock-stall problems, e.g. Harrier, Blackburn Buccaneer, Gloster Javelin [4]. The purpose of this research work is to experimentally observe the pressure distribution over the surface of an airfoil NACA 4215 with and without flaps at different flap angles also by momentum injection.

II. Model Construction

The airfoil coordinates of NACA 4215 are generated by using the following formulas;

Parameter calculation: [5], [6]

Leading Edge Radius, $r = 1.1019t^2$

Half thickness distribution,

$$y_t = 5t\left(0.2969\sqrt{x} - 0.1260x - 0.3516x^2 + 0.2843x^3 - 0.1015x^4 \right) \quad (3)$$

where x is the position along chord from 0 to 1 ($i.e. 0 \le x \le 100\%$). Mean camber line,

$$y_c = \begin{cases} \frac{m}{p^2}(2px - x^2) & 0 \le x \le p \\ \frac{m}{(1-p)^2}[(1-2p) + 2px - x^2] & p \le x \le c \end{cases} \quad (4)$$

The slope of the camber line at any point x,

$$\left.\frac{dy_c}{dx}\right|_x = \begin{cases} \frac{2m}{p^2}(p - x) & 0 \le x \le p \\ \frac{2m}{(1-p)^2}(p - x) & p \le x \le c \end{cases} \quad (5)$$

$$\tan\theta = \left.\frac{dy_c}{dx}\right|_x \quad \therefore \theta = \tan^{-1}\left(\frac{dy_c}{dx}\right) \quad (6)$$

The upper surface coordinates,

$$x_u = x - y_t \sin\theta \quad (7)$$

$$y_u = y_c + y_t \cos\theta \quad (8)$$

The corresponding expressions for the lower surface coordinates:

$$x_L = x + y_t \sin\theta \quad (9)$$

$$y_L = y_c - y_t \cos\theta \quad (10)$$

Coordinate Generation of NACA 4215 Airfoil:

$$c = 20\ cm$$
$$m = 0.04c = 0.04 \times 20 = 0.8\ cm$$
$$p = 0.2c = 0.2 \times 20 = 4\ cm$$
$$t = 0.15c = 0.15 \times 20 = 3\ cm$$
$$\therefore r = 1.1019t^2 = 1.1019(0.15)^2 = 0.024\ cm$$

Traditionally, the outline of an airfoil is plotted XY plane. On the left at (X=0,Y=0) Is placed the point corresponding to the wing leading edge. This part of the airfoil is usually rounded. The radius of this curvature is often given on the drawing, as additional information. The other end of the outline is always placed at the trailing edge (X = 100, Y = 0). The other end of the outline is always placed at the trailing edge (X = 100, Y = 0). The contour of the airfoil can be divided into two parts: the upper and the lower. They joined at their ends (X=100, Y=0). After plotting the upper and lower coordinates we get the section of NACA 4215 airfoil.

The experiments were conducted in the test section of an open circuit wind tunnel shown in Fig. 5 where a uniform and steady velocity field is established. The wind tunnel is suction type and the honeycomb section contraction type and the test section flow field is fully developed. Also, we tested the mirror effect which is around 15% of the length that means the central 70% area is fully uniform flow. And the velocity of wind changes by using a variable transformer that is connected with A/C motor, and velocity change is very smooth. The wind tunnel is approximately 7.35 m long, and the test section is a 0.90 m by 0.90 m square, 1.35 m long. The facility enables measurements for the flow velocity up to 40 m/s. A photograph of the tunnel contraction housing the test platform is provided in Fig. 5.

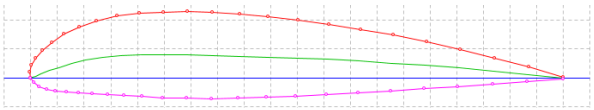

Fig. 1 NACA 4215 section profile based on airfoil section CAD design (using solid works 2013) are given below. For model 2 and model 3 the length of flap is 0.3C

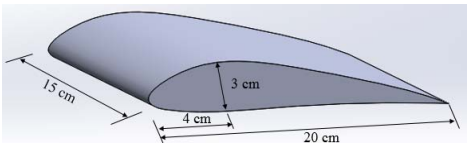

Fig. 2 CAD design of NACA 4215 (Model 1)

Fig. 3 CAD design of NACA 4215 with trailing edge flap (Model 2)

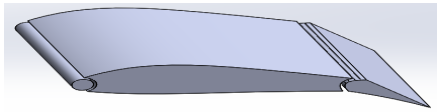

Fig. 4 CAD design of NACA 4215 with leading edge rotating cylinder and trailing edge flap (Model 3)

Fig. 5 Wind tunnel in Aerodynamics Lab, KUET

To measure the static surface pressure of the airfoil, an automatic data acquisition system has been used. Pressure probes were attached on the surface of the model. The pressure probes and pressure sensor were connected by vinyl tube with 1.0 mm internal diameter and 3 m long. Customized Student version LabView-based software was used to interface the data acquisition system. ADAS contains several

measurement modules: pressure distribution, velocity around the airfoil, load cell etc. To measure the free stream velocity of the tunnel test section, a standard digital pitot tube was used. In the experiment, the *Re* numbers change by changing the free stream velocity and free stream velocity controlled by motor transformer interface. The pressure data were automatically saved in the computer by average value of 50 Hz.

III. Experimental Results and Discussion

The wooden airfoil model are tested in following conditions: $P_\infty = 101325\ Pa;\ V_\infty = 30\ m/s;\ \rho_\infty = \rho_{air} = 1.225\ m^3/kg;\ \mu_{air} = 1.81 \times 10^{-5}\ Pa.s; T = 28℃ = 301\ K$. The local flow Reynolds number is $R_e = 1.83 \times 10^6$ and Mach number is $M = 0.8655$ (see sample calculation Appendix). So, the flow is subsonic. The aerodynamic characteristics are calculated for seven angles of attack $0°, 4°, 8°, 10°, 12°, 14°\ and\ 16°$. The pressure coefficient vs. chord length graph is combined for three models which help us to analyze the variation pressure over airfoil for various arrangement. Theses graph are given below.

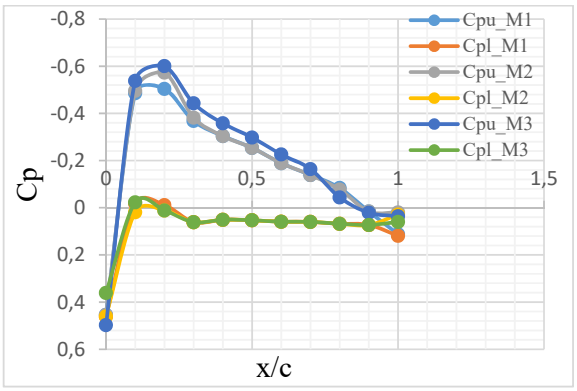

Fig. 6 Comparison of pressure coefficient (C_p) distribution along chord (x/c) at α = 0°

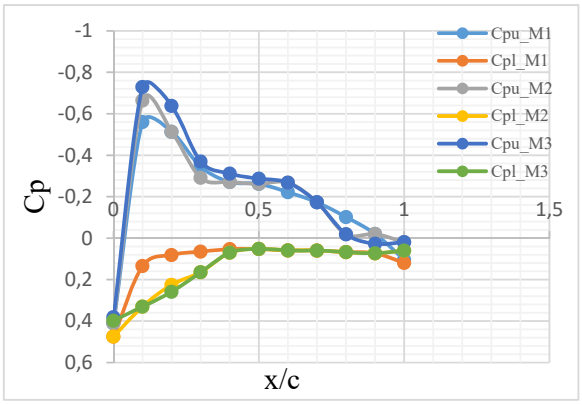

Fig. 7 Comparison of pressure coefficient (C_p) distribution along chord (x/c) at α = 4°

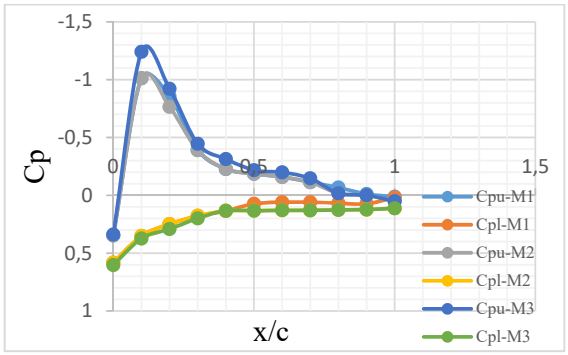

Fig. 8 Comparison of pressure coefficient (C_p) distribution along chord (x/c) at α = 8°

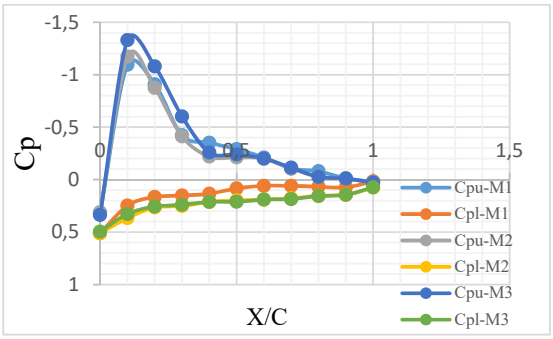

Fig. 9 Comparison of pressure coefficient (C_p) distribution along chord (x/c) at α = 10°

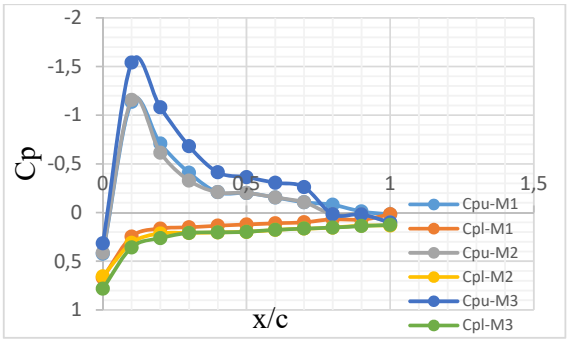

Fig. 10 Comparison of pressure coefficient (C_p) distribution along chord (x/c) at α = 12°

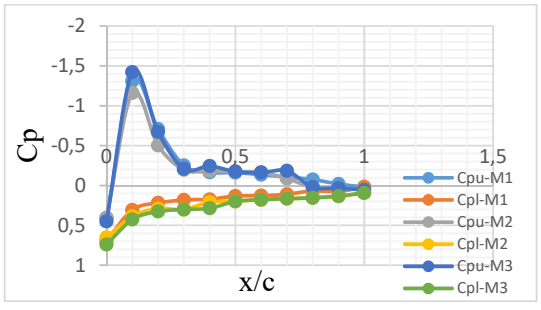

Fig. 11 Comparison of pressure coefficient (C_p) distribution along chord (x/c) at α = 14°

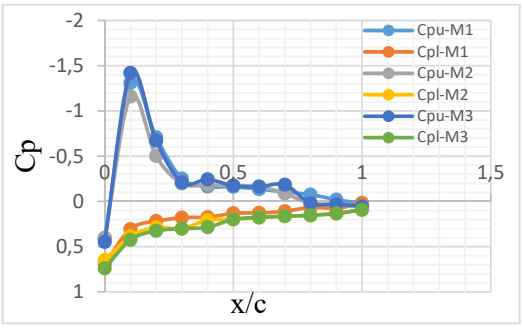

Fig. 12 Comparison of pressure coefficient (C_p) distribution along chord (x/c) at $\alpha = 16°$

The experimental results of surface pressure distributions are shown in Figs. 1-6 for simple NACA 4215 airfoil, with flap and with leading edge rotating cylinder model. As shown in the figures, there is no flow separation which occurs for all models at zero attack angle. As the attack angle increased from 0° to 10°, flow separation occurs as shown in model 1 (simple NACA 4215 airfoil). For this model, at the point of 10°AOA, we achieve maximum lift coefficient. As the attack angle increased from 10° to 16°, flow separation appeared on the upper surface and lift coefficient decrease gradually. For model 2 (NACA 4215 with flap), lift coefficient shows previous characteristic but in this case lift coefficient increases by 12.5%, so one of our goal which is to increase lift is achieved. Maximum lift occurs at around 12° AOA, beyond this, stall criteria happen and lift decreases. For model 3 (NACA 4215 with flap and rotating cylinder at leading edge) where momentum is injected at a rate 9.773, stall is delayed and it happens at 14° AOA so our objective is achieved.

IV. Conclusion

From the experimental investigations, it has been observed that the flow separation on the airfoil can be delayed by 3-5% of chord length by using the momentum injection technique on the upper surface. Flow separation occurs at 10° angle of attack in the simple NACA 4215 airfoil, but in momentum injected surface, it occurs at 14° angle of attack. That indicates the momentum injection technique controls the flow separation and improve the performance of the wing.

References

[1] A. L. Braslow, A history of suction-type laminar-flow control with emphasis on flight Research, Monographs in Aerospace History #13, NASA History Division Office of Policy and Plans, NASA Headquarters Washington, DC 205469,1999.
[2] A. Seifert, T. Bachar, D. Koss, M. Shepshelovich, and I. Wygnanski, Oscillatory blowing: A tool to delay boundary-layer separation, AIAA Journal, 31(11), 1993.
[3] L. M. M. Boermans, Glide ratio 1:80, A solar challenge?, Paper at XXV OSTIV Congress St. Auban, France, 1997.
[4] J. Little, M. Nishihara, I. Adamovich, and M. Samimiy. Separation control from the flap of a high-liftairfoil using DBD plasma actuators. In AIAA Paper 2009 145, 2009.
[5] John D. Anderson Jr Fundamentals of Aerodynamics., 5th Edition, Mc-Graw Hill, December 2009.
[6] John D. Anderson Jr. (2012), Introduction to Flight, 7th Edition, Mc-Graw Hill, August 2011.